Do Protein Molecules Unfold in a Simple Shear Flow?

Juan Jaspe and Stephen J. Hagen
Department of Physics, University of Florida, Gainesville, Florida

ABSTRACT Protein molecules typically unfold (denature) when subjected to extremes of heat, cold, pH, solvent composition, or mechanical stress. One might expect that shearing forces induced by a nonuniform fluid flow would also destabilize proteins, as when a protein solution flows rapidly through a narrow channel. However, although the protein literature contains many references to shear denaturation, we find little quantitative evidence for the phenomenon. We have investigated whether a high shear can destabilize a small globular protein to any measurable extent. We study a protein (horse cytochrome *c,* 104 amino acids) whose fluorescence increases sharply upon unfolding. By forcing the sample through a silica capillary (inner diameter 150–180 μm) at speeds approaching 10 m/s, we subject the protein to shear rates dv_z/dr as large as $\sim 2 \times 10^5$ s^{-1} while illuminating it with an ultraviolet laser. We can readily detect fluorescence changes of $<1\%$, corresponding to shifts of $<\sim 0.01$ kJ/mol in the stability of the folded state. We find no evidence that even our highest shear rates significantly destabilize the folded protein. A simple model suggests that extraordinary shear rates, $\sim 10^7$ s^{-1}, would be required to denature typical small, globular proteins in water.

INTRODUCTION

The effects of many kinds of solvent conditions and parameters on the thermodynamic stability of protein molecules have been investigated in depth. Ions and cosolutes, extremes of temperature and pH, chaotropic agents (urea and guanidinium ion), surfactants, surface forces, dehydration, and even mechanical forces are all capable of stabilizing or destabilizing the folded state of a protein, and these effects have been explored for a large number of biologically and technologically important proteins (1). It is also widely believed that shear stresses arising from fluid flow can affect protein stability (2,3): since proteins are polymer chains, pumping or filtration processes that subject a protein solution to large velocity gradients are often described as capable of deforming or denaturing (unfolding) the native structure of the protein, resulting in aggregation, loss of enzyme activity, or even fragmentation of the covalent backbone. Although this presents a problem in the handling and processing of proteins in biotechnology applications, it would also present a scientific opportunity if it allowed researchers to use shear denaturation as a probe of protein dynamics: researchers could build microfluidic devices that use shearing forces to trigger the unfolding and refolding of proteins, complementing other triggers (rapid mixing, photochemistry, laser heating, etc.) in current use.

However, although references to shear denaturation appear frequently in the protein literature, the experimental evidence for the phenomenon is often either indirect or complicated by the experimental design. In short, the literature contains a number of conflicting and somewhat confusing reports. Many early studies subjected proteins to poorly controlled shear conditions, such as filtration or rapid stirring, in which the velocity gradients were heterogeneous (in both space and time) and difficult to quantify. Shear is often applied for prolonged periods, with the result that cumulative effects are observed; these may reflect gradual surface denaturation or aggregation as well as the consequences of shear. Further, denaturation is often probed through enzyme activity assays that, although capable of detecting irreversible denaturation and aggregation, lack the sensitivity and time resolution of optical spectroscopic probes of protein conformation. Removing the protein from the shearing flow to measure enzyme activity may in some cases have allowed the protein to refold before measurement. Therefore, the question of whether proteins really do unfold in commonly attainable shear flows has remained unclear, despite the obvious practical implications of shear flow for industrial biopharmaceutical and microfluidic applications. We have attempted to answer this question by subjecting a well-characterized protein to high rates of shear under controlled conditions where we can use a sensitive probe (fluorescence spectroscopy) to detect even small degrees of unfolding as the shear is applied. We present experimental results along with a simple theoretical perspective on shear denaturation.

Earlier studies examined the effect of either high shear rate $\dot{\gamma}$, shear γ, or shear stress σ on protein stability. For laminar fluid flow through a cylindrical channel of radius R, the fluid velocity v_z is a function of distance r from the cylindrical (z) axis (4):

$$v_z(r) = \frac{1}{4\eta}\frac{\partial P}{\partial z}(R^2 - r^2), \tag{1}$$

where η is the dynamical viscosity of the fluid and $P(z)$ is the hydrostatic pressure. The shear rate $\dot{\gamma}$ is the radial derivative of the velocity v_z,

$$\dot{\gamma}(r) = \left|\frac{dv_z}{dr}\right| = \frac{r}{2\eta}\frac{\partial P}{\partial z},$$

Submitted May 17, 2006, and accepted for publication July 17, 2006.

Address reprint requests to Stephen J. Hagen, University of Florida, Physics Department, Museum Road and Lemerand Drive, PO Box 118440, Gainesville, FL 32611-8440. Tel.: 352-392-4716; E-mail: sjhagen@ufl.edu.

0006-3495/06/11/3415/10 $2.00

doi: 10.1529/biophysj.106.089367

and is a function of r. The shear or strain history, $\gamma = \dot{\gamma}t$, is a dimensionless measure of the amount of time t that a sample has been exposed to a velocity gradient. The shear stress, $\sigma = \eta\dot{\gamma}$ is perhaps the better indicator of the actual denaturing force acting on the protein; in fact, most (but not all (5)) shear denaturation studies have used aqueous solvents, for which $\eta \approx 10^{-3}$ Pa s.

Early reports (6–11) suggested that several enzymes, including fibrinogen, urease, rennet, and catalase, begin to lose activity after exposure to shear $\gamma > \sim 10^4$–10^5, even at relatively low shear rates, $\dot{\gamma} \sim 10\ s^{-1}$ (6,7). However, later studies of alcohol dehydrogenase, catalase, and urease (12, 13) found little or no evidence for shear deactivation of these enzymes, even for $\gamma \sim 7 \times 10^6$ and $\dot{\gamma} \sim 700\ s^{-1}$. These conflicting results raised the question of whether the enzymes in the earlier studies were actually denaturing through an interaction with an air-liquid interface or with a solid surface, rather than as a consequence of shear. Subsequent studies confirm that surface denaturation can be the more important mechanism: $\dot{\gamma} \sim 10^5\ s^{-1}$ and $\gamma \sim 10^6$ had negligible denaturing effects on human growth hormone (14, 15). Nevertheless, those same authors also described some evidence of permanent changes in the protein after prolonged shearing, including changes in the melting temperature, as well as possible breakage of peptide bonds. This implies that at least some transient unfolding did occur. Force microscopy imaging of a very large plasma glycoprotein (vWF, a multimeric enzyme with molecular weight as large as 2×10^7) adhering to a surface seemed to reveal a shear-induced conformational transition (although not necessarily unfolding) occurring at a shear stress $\sigma = \eta\dot{\gamma} \approx 3.5$ Pa (16), or $\dot{\gamma} = \sigma/\eta \approx 3.5 \times 10^3 s^{-1}$. In one of the most careful studies in this area, Lee and McHugh investigated the effect of simple shear on the helix-coil transition of poly-L-lysine (17). For solvent conditions that placed the sample very near the midpoint of its equilibrium helix-coil transition, they observed loss of helicity occurring at a critical shear rate $\dot{\gamma} \sim$ 300–400 s^{-1} in a Couette flow cell. This provided convincing evidence that simple shear can influence the unfolding equilibrium in a polypeptide; it did not however reveal the value of $\dot{\gamma}$ that is needed to denature a small globular protein. However, an α-amylase of 483 amino acids was partially deactivated by simple shear at stresses $\sigma > 3 \times 10^4$ Pa in a highly viscous medium (5) (although at modest $\dot{\gamma} \sim$ 120 s^{-1}); this value of σ suggests that a phenomenal shear rate $\dot{\gamma} \sim 10^7\ s^{-1}$ would have been required to denature the protein in water ($\eta \approx 10^{-3}$ Pa s). In any case, despite the somewhat confusing experimental situation, concerns about shear denaturation persist in the protein physical chemistry and biotechnology literature (2) and the topic arises regularly in basic research in a wide area of protein science, including enzyme kinetics (18), protein molecular dynamics (19), and microrheology (20).

We have investigated the effect of high rates of shear on ferric equine cytochrome c, a 104-residue globular protein whose equilibrium and kinetic folding properties (in the absence of shear) have been extremely well characterized previously by many authors. Because both folding and unfolding of cytochrome c is rapid (timescales of approximately microseconds to milliseconds) and fully reversible (21), we expect that the protein, if unfolded by high shear in a narrow channel, will successfully refold once it exits the channel. It seems very unlikely that multiple passes through the capillary will have any cumulative or delayed denaturing effect, as was imagined in some early denaturation studies. Therefore, it is necessary to test for unfolding while the protein remains in the shearing flow. We pump the protein solution through a narrow, transparent capillary and use fluorescence microscopy to probe the folding/unfolding equilibrium of the protein as it travels through the capillary.

Cytochrome c contains a natural fluorophore, a single tryptophan residue at position 59 (i.e., Trp-59), that responds dramatically to the folding/unfolding transition of the protein (Fig. 1). In the folded state, the fluorescence of the Trp-59 indole side chain is strongly quenched because of its proximity to the heme (distance 0.94 nm), an iron-porphyrin group that is covalently attached to the polypeptide chain by cysteine residues Cys-14 and Cys-17, and by histidine His-18. This quenching occurs through the distance-sensitive Forster mechanism (22). When the protein unfolds, the expansion of the chain increases the average distance between Trp-59 and the heme toward a value comparable to the

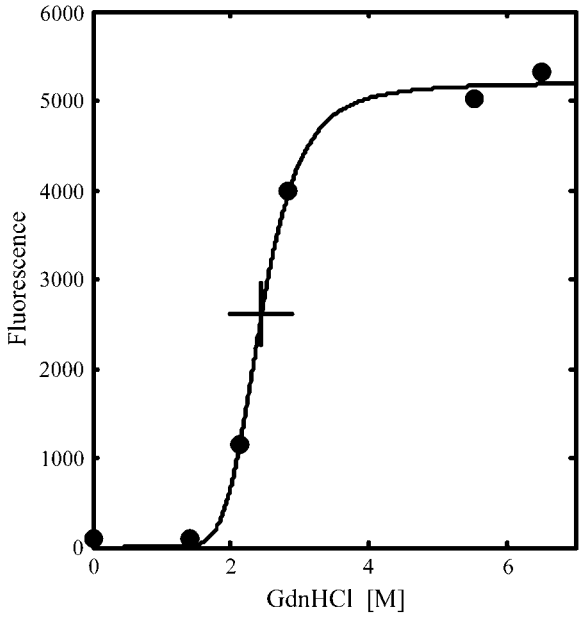

FIGURE 1 Equilibrium fluorescence of ferric cytochrome c versus GdnHCl concentration at 25°C, pH 5.0, showing the denaturant-induced unfolding transition. Solid circles are the wavelength-integrated fluorescence emission (measured with 266-nm excitation); solid curve is a fit to a simple two-state unfolding model where the unfolding free energy is $\Delta G = \Delta G_0 - m$[GdnHCl]; *solid cross*, transition midpoint where $\Delta G = 0$ (at 2.5 M GdnHCl).

Forster radius $R_0 = 3.2$ nm, leading to reduced energy transfer and a $\sim 10^2\times$ increase in fluorescent emission by the protein. We excite the tryptophan fluorescence with a laser ($\lambda = 266$ nm) while the protein flows through a narrow silica capillary at high velocity; by collecting the fluorescent emission ($\sim$350 nm) with a photomultiplier we can detect small changes in fluorescence, revealing even small amounts of transient unfolding in response to the shear flow.

MATERIALS AND METHODS

We performed all experiments at 25°C, with the cytochrome *c* dissolved in denaturant/buffer solutions at pH 7.0 and pH 5.0. We found the same results at both the neutral and acidic pH, although here we present only the pH 5.0 data. Working at pH 5 instead of pH 7 does not greatly affect the folding equilibrium of cytochrome *c*: It shifts the denaturation midpoint to (approximately) 2.5 M guanidine hydrochloride (GdnHCl) from the pH 7 value of $\sim$2.8 M GdnHCl at 25°C. This shift is due to a reduction in the folding stability in water (ΔG_0) from 42.4 kJ/mol to 38.3 kJ/mol at 25°C, i.e., by $\sim$10% (23). However, pH 7.0 is a less desirable experimental condition for folding studies of cytochrome *c* because the histidine residues His-26 and His-33 can bind transiently to the heme iron during folding; this generates an additional (but largely uninteresting) kinetic phase in folding experiments at neutral pH (21,23,24). At lower pH, those residues become protonated (pK $\approx$ 5.7) and cannot bind to the heme, so that at pH 5.0 the additional kinetic phase is largely suppressed and simpler folding kinetics are observed (23).

We dissolved lyophilized equine ferricytochrome *c* (type C7752, Sigma-Aldrich, St. Louis, MO) at 40–50 μM in 25 mM citric acid buffer, pH 5.0, that also contained GdnHCl at a concentration of either 2.47 M or 1.36 M. For control measurements, we prepared 50 μM free tryptophan (*N*-acetyl-L-tryptophanamide, or NATA) in the same GdnHCl/citric acid buffers. GdnHCl concentrations were determined refractometrically. Solvent dynamic viscosities η were obtained from tabulated values at 25°C (25).

Fig. 2 shows the sample flow scheme. Each solution was loaded into a plastic vial and pumped by N_2 pressure through flexible Tygon tubing (inner diameter (ID) 1/16 inches) leading to a syringe needle. A narrow-bore, cylindrical-fused silica capillary (Polymicro Technologies, Phoenix, AZ) was cemented into the tip of the syringe needle. We used two different sizes of silica capillary tubing (see Table 1): capillary 1 (for 2.47 M GdnHCl) had inner radius $R = 75$ μm, outer diameter 360 μm, and length $L = 24$ mm, and capillary 2 (for 1.36 M GdnHCl) had $R = 90$ μm, outer diameter 340 μm, and $L = 25$ mm. The high fluid velocity (up to $\sim$10 m/s) inside the narrow capillary resulted in strong shear ($\dot{\gamma} \sim 10^5$ s^{-1}), while the ultraviolet (UV)-visible optical transparency of the silica allowed us to probe the tryptophan fluorescence of the protein. After passing through the capillary, the sample entered a second syringe needle and returned (via additional tubing) to a storage vial.

Calculations indicated that flow in both capillaries would be laminar (not turbulent) for our experiments, and that pressure losses in the supply and return tubing would be minimal. We confirmed this by measuring the rate of volume flow, Q (m^3/s), through both capillaries. For each capillary, we connected the output tubing to a 5-ml volumetric flask and then used a stopwatch to measure the time required to fill the flask at various pressures. Such measurements of Q were reproducible to $\pm$2–3%. We compared these measurements with the expected (i.e., Hagen-Poiseuille law) rate Q of laminar, stationary fluid flow through a cylindrical channel (4),

$$Q = \frac{\pi R^4}{8\eta}\frac{dP(z)}{dz} = \frac{\pi R^4 \Delta P}{8\eta L}, \qquad (2)$$

where $P(z)$ is the hydrostatic pressure, ΔP is the hydrostatic pressure drop across the length L of the capillary, and η is the dynamic viscosity. Equation 2 predicts $Q/\Delta P \approx 4.84 \times 10^{-7}$ ml/s/Pa and 1.00×10^{-6} ml/s/Pa for capillaries 1 and 2, respectively. Fig. 3 shows that the measured values were 4.6×10^{-7} ml/s/Pa and 0.91×10^{-6} ml/s/Pa for these capillaries (see Table). The very satisfactory agreement of these measured values with Eq. 2 and the linearity of the measured Q versus ΔP together indicate that neither turbulence nor pressure losses in the supply or return tubing affected the flow significantly.

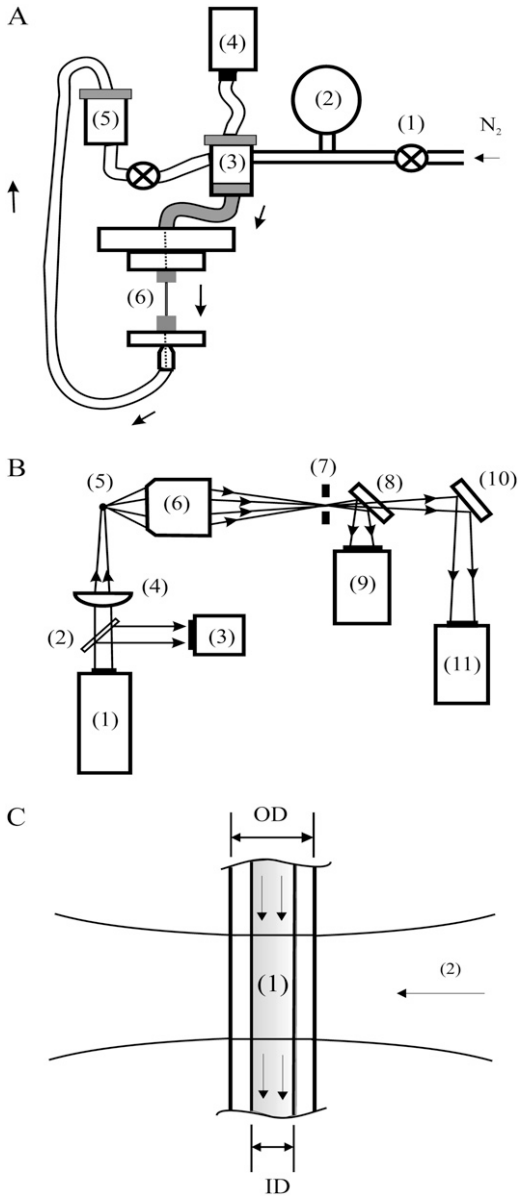

FIGURE 2 (*A*) Flow apparatus for shear denaturation measurement: (*1*) N_2 pressure regulator; (*2*) monitoring pressure gauge; (*3*) sample reservoir; (*4*) digitizing pressure gauge (connected to computer); (*5*) sample return reservoir; and (*6*) fused silica capillary. (*B*) Fluorescence excitation and detection apparatus: (*1*) UV laser ($\lambda = 266$ nm); (*2*) beam splitter; (*3*) reference photodiode; (*4*) converging lens ($f = 15$ mm); (*5*) fused silica capillary, axial view; (*6*) microscope objective (10×/0.3 NA) with long-pass Schott glass filter; (*7*) iris; (*8*) beam splitter; (*9*) CCD monitoring camera; (*10*) mirror; (*11*) photomultiplier. (*C*) Laser illumination of capillary: (*1*) channel containing sample flow; (*2*) UV laser beam brought to weak focus at capillary. capillary inner (*ID*) and outer (*OD*) diameters are indicated.

TABLE 1 Geometrical and flow parameters for flow capillaries

Parameter	Expression	Capillary 1	Capillary 2	Units
Inner radius	**R**	75	90	μm
Outer radius	—	180	170	μm
Length	**L**	24	25	mm
$Q/\Delta P$	$\pi R^4/8\eta$	4.84×10^{-7}	1.00×10^{-6}	ml/s/Pa
$Q/\Delta P$	(Measured)	4.6×10^{-7}	0.91×10^{-6}	ml/s/Pa
Q_{max}	(Measured)	0.0785	0.153	ml/s
$\langle\dot{\gamma}\rangle$	$8Q_{max}/3\ \pi R^3$	1.58×10^5	1.78×10^5	s^{-1}
v_{max}	$2Q_{max}/\pi R^2$	8.8	12	m/s
$\langle v_{max}\rangle$	$Q_{max}/\pi R^2$	4.4	6.0	m/s
$L/\langle v_{max}\rangle$	$\pi R^2 L/Q_{max}$	0.0054	0.0042	s
max(Re)	$\rho V_{max} R/\eta$	660	1150	—

Capillary 1 was used for experiments at 2.46 M GdnHCl and capillary 2 was used for experiments at 1.36 M GdnHCl. Q is the rate of volume flow, ΔP is the driving pressure, v is the velocity of flow, Re is the Reynolds number, ρ is the fluid density, and brackets indicate averages over r within the capillary.

We used a 266-nm quasi-CW laser (2 mW, NanoUV, JDS Uniphase, Milpitas, CA) to excite the fluorescence of the tryptophan in the samples flowing in the capillary (Fig. 2). A manual pressure regulator (Omega Engineering, Stamford, CT) was adjusted to vary the N_2 driving pressure in the sample reservoir slowly, up to values as large as 26.3 psi $= 1.8 \times 10^5$ Pa (relative to atmosphere), while an electronic pressure gauge (SPER Scientific, Scottsdale, AZ) sent the pressure data to a computer. A silica lens ($f =$ 15 mm) brought the UV laser beam to a slightly defocused spot (just wider than the capillary outer diameter, ~340–360 μm) on the capillary, so as to illuminate uniformly all the fluid in the channel, at the midpoint of the capillary (Fig. 2). A microscope objective collected the fluorescence emission from the sample during the pressure scan and directed it onto an iris that limited the width of the detection volume to 0.4 mm, or roughly the capillary OD. Emitted light then passed to a photomultiplier detector (type R1166, Hamamatsu Photonics, Bridgewater, NJ), whose signal was recorded by a digitizing oscilloscope and transmitted to the computer. We verified that the photomultiplier signal was linear in the sample fluorescence. Owing to large differences in the equilibrium fluorescence of the protein samples under different solvent conditions (see Fig. 1), it was necessary to adjust the photomultiplier bias voltage for each different sample, keeping the output signal level at roughly the same value (~50 mV). This maintained detector linearity and prevented damage to the detector.

Data for both protein and control (NATA) samples were collected and compared under identical solvent and flow conditions. The data in the figures represent an average of (typically) 10 pressure scans, each lasting ~80 s and using ~10–12 ml of solution. For each measurement, we determined the fluid flow rate Q from the product of the applied N_2 pressure ΔP and the measured value of the capillary's $Q/\Delta P$ ratio. The Reynolds number Re did not exceed ~1100 during any measurements.

As discussed above, the fluid velocity v_z and the shear rate in the capillary are both functions of radius r. Different protein molecules experience different shear. Because we are looking for a threshhold effect—i.e., does any measurable denaturation occur at large shear?—we illuminate the entire flow volume ($r = 0 \rightarrow R$) and look for a flow-rate dependence of the fluorescence emission. Owing to the cylindrical geometry, most of the volume in the capillary lies closer to the walls, where the shear rate is largest: This part of the sample dominates the signal. Since the shear rate is nonuniform in the probed volume, the figures below present the measured fluorescence as a function of the average shear rate (i.e., averaged over the channel cross section):

$$\langle\dot{\gamma}\rangle = \frac{1}{\pi R^2}\int_0^{2\pi} d\theta \int_0^R r dr\, \dot{\gamma}(r) = \frac{\partial P}{\partial z}\frac{R}{3\eta} = \frac{8Q}{3\pi R^3}.$$

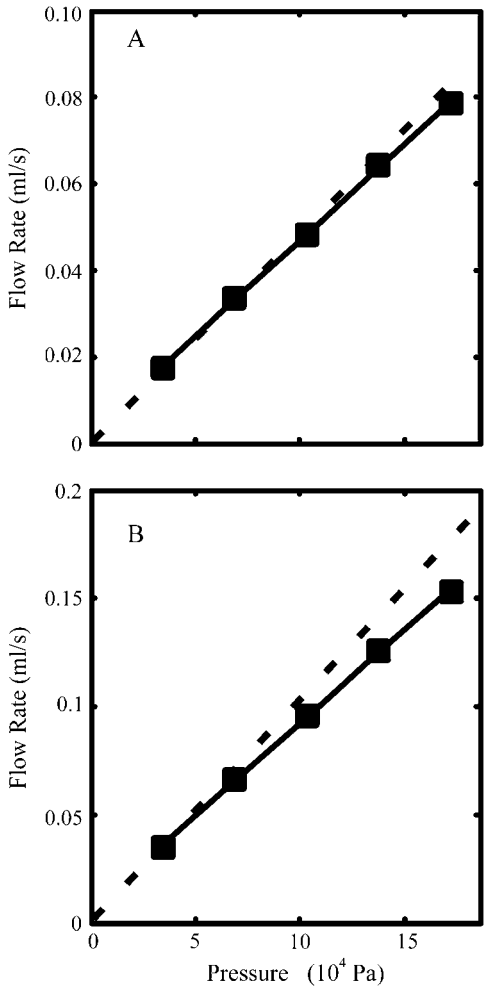

FIGURE 3 Calibration of flow rates in capillaries 1 (*A*) and 2 (*B*): Solid points are measured flow rates at the pressures ΔP indicated; solid line is the fit to a straight line $Q \propto \Delta P$; dashed line is the prediction of Eq. 2. Parameters are given in Table 1.

RESULTS AND DISCUSSION

We first examine the effect of high shear on the protein under very slightly destabilizing conditions, 1.36 M GdnHCl, where the native state remains stable but enough unfolded molecules are present to generate a fluorescence signal. For this solvent, we estimate the free energy of unfolding is $\Delta G \approx 17.5$ kJ/mol or $\Delta G/k_BT \approx 7.06$ (based on the denaturation midpoint 2.5 M GdnHCl and the GdnHCl dependence of the unfolding free energy, $m = 15.3$ kJ/mol/M at 25°C (23,26)). In a two-state unfolding model, where the fluorescence emission F is virtually all due to the unfolded molecules,

$$F \propto (1 + \exp(\Delta G/k_BT))^{-1}.$$

Then, for our fairly large $\Delta G/k_BT$ we have $d\log F/d\log\Delta G \approx -\Delta G/k_BT \approx -7$. If the effect of shear is to reduce ΔG by, e.g., 1%, we expect a fluorescence increase $d\log F \sim (-0.01) \times (-7) = 7\%$. Fig. 4 shows the fluorescence of both the

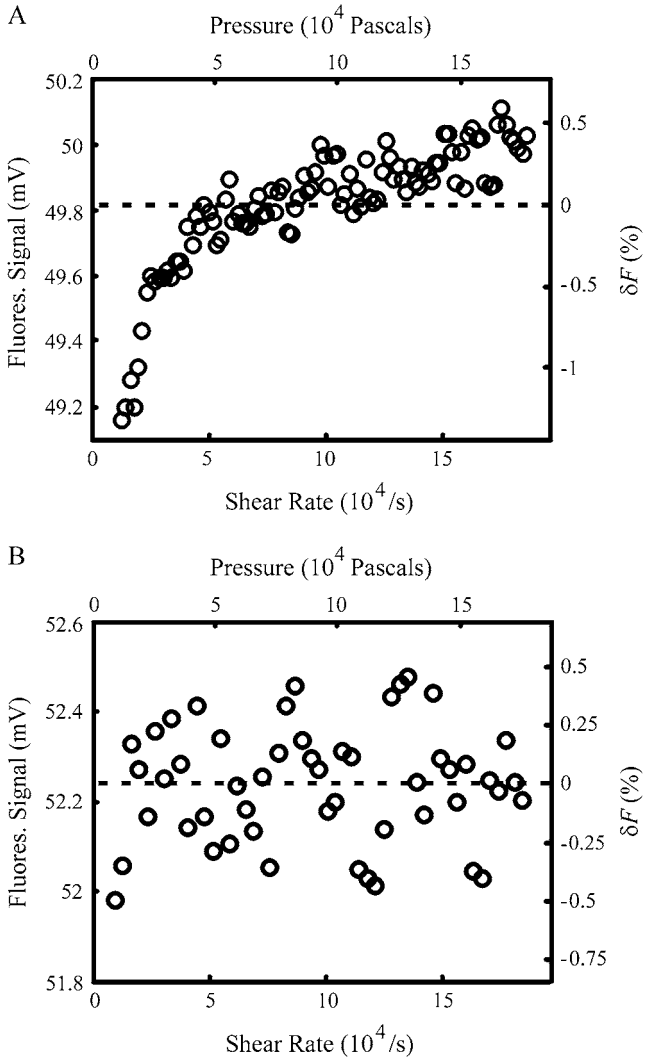

FIGURE 4 Fluorescence of (*A*) tryptophan (NATA) control and (*B*) cytochrome *c*, versus applied driving pressure and volume-averaged shear rate $\langle\dot{\gamma}\rangle$. Both samples are in 1.36 M GdnHCl, pH 5.0, citric acid buffer.

protein and the tryptophan (NATA) control samples over a range of shear rates. The rise in the fluorescence of the control can be attributed to photobleaching (see below). For the cytochrome *c*, the fluorescence *F* remains essentially constant, scattered around its mean value with a standard deviation of ≈0.3%, from $\langle\dot{\gamma}\rangle = 0$ to $\langle\dot{\gamma}\rangle = 1.8 \times 10^5\ s^{-1}$. The absence of a more substantial rise in the sample fluorescence indicates that even the maximum shear rate does not shift the stability ΔG by more than ≈(1/7) × (.3%) ~ 0.04% or 0.0075 kJ/mol ≈ 0.003 k_BT.

Of course, it is also possible that the high shear rate destabilizes the native state but the protein does not remain in the capillary for sufficient time to allow the folded and unfolded populations to reach a new equilibrium. The timescale for a protein molecule to travel the length of the capillary is approximated by the ratio of the capillary length *L* to the (volume averaged) flow velocity, $\langle v\rangle$. For this capillary (capillary 2), the residence time is $L/\langle v_{max}\rangle \approx 4.2$ ms at the maximum shear rate, and proportionally longer at lower shear rates. By comparison, the folding/unfolding relaxation in this solvent is expected to occur at a rate $<\sim 300\ s^{-1} \approx (3.3\ ms)^{-1}$ (21). This implies that whereas the protein had sufficient time to denature while flowing at lower shear rates —and evidently did not do so—it may not have had sufficient time to unfold at the highest shear rates.

The above two-state view of cytochrome *c* folding therefore provides some evidence against shear denaturation. However, it is useful to employ a more complete description of cytochrome *c* folding. Through a series of ultrafast mixing studies, Roder and others established a three-state chemical kinetic scheme for the folding of cytochrome *c* (Fig. 5) (21).

Here, *N* is the nonfluorescent, native (i.e., folded) state and *U* is the expanded, highly fluorescent unfolded state. *I* is a compact, ''molten-globule'' intermediate state of native-like (i.e., low) fluorescence. Interconversion between *I* and *N* does not greatly affect either the dimensions or the fluorescence of the molecule: one would not expect this interconversion to be driven by high shear rates, or to be detectable with our experimental probe. By contrast, reequilibration between *I* and *U* involves expansion of the chain and, consequently, a large (i.e., detectable) fluorescence change, and is presumably more likely to respond to a shear flow. It should therefore be advantageous to select solvent conditions that maximize the *I* population, and then apply a high shear rate to shift the $I \rightarrow U$ equilibrium.

The populations of *N*, *I*, and *U* as a function of denaturant can be calculated from the Roder et al. estimates for the underlying rates k_{IU}, k_{NI}, etc., and from published equilibrium data (26). The result is similar to the results of a three-state analysis of small angle x-ray scattering data for cytochrome *c* (27). Essentially, the fraction of molecules occupying state *I* is always relatively small, but reaches its maximum (~10%, based on the rate data of Roder et al.) near the midpoint of the *N*-*U* unfolding transition, at 2.8 M GdnHCl (pH 7). Making a small correction for the slightly reduced stability of *N* at lower pH, we then expect the

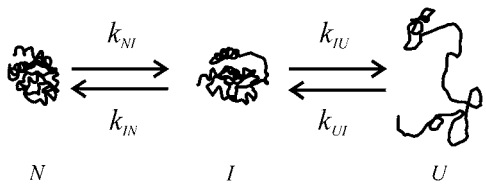

FIGURE 5 Three-state kinetic model for cytochrome *c* folding, derived by Roder and coworkers from rapid mixing studies (21). The compact, nonfluorescent native state *N* and intermediate *I* interconvert slowly (roughly milliseconds). Interconversion between the intermediate *I* and the fluorescent, strongly unfolded state *U* proceeds more rapidly (roughly microseconds).

maximum population of N at pH 5.0 to occur near 2.5 M GdnHCl (again the midpoint of the unfolding transition).

Therefore, we tested for shear denaturation of cytochrome c at this solvent condition (pH 5.0, 2.47 M GdnHCl). Here, the rate of the equilibration N-I is relatively slow, $k \approx k_{NI} + k_{IN} \approx 100\ s^{-1} = (10\ ms)^{-1}$. The important I-U equilibration, however, occurs at a very rapid rate, $k \approx k_{UI} + k_{IU} > 2 \times 10^4\ s^{-1} = (50\ \mu s)^{-1}$ (21). Even at our maximum flow rates, the characteristic residence time of the protein in the capillary ($L/\langle v_{max} \rangle = 5.4$ ms) is ample for this rapid process to equilibrate.

Fig. 6 shows the results under these conditions: the behavior of the cytochrome c and the control sample are quite similar. In the control sample (i.e., NATA or free tryptophan) (Fig. 6, *upper*), the fluorescence first increases quite steeply as the flow begins and the pressure rises to $\sim 3 \times 10^4$ Pa, where the shear rate is $\langle \dot{\gamma} \rangle \approx 2.5 \times 10^4\ s^{-1}$. As the flow rate rises further, toward $\langle \dot{\gamma} \rangle \approx 1.6 \times 10^5\ s^{-1}$, the fluorescence shows a slight (<1%) additional rise. Although one does not expect the fluorescence of the control to depend on flow rate, this is most probably the signature of photobleaching: tryptophan is known for its very poor photostability. The Appendix demonstrates that the fluorescence data in Fig. 6 is affected by photobleaching at the very lowest flow rates, where the sample resides for many milliseconds in the beam focus. At moderate and high flow rates the sample spends little time in the focus and the fluorescence is less sensitive to flow rate, although a slight upward trend remains at high flow rates. The protein sample (Fig. 6, *lower*) shows essentially the same behavior as the control. It does exhibit a possible weak maximum near $\langle \dot{\gamma} \rangle \approx 1.4 \times 10^5\ s^{-1}$, but that is unlikely to be a signature of shear denaturation: unfolding corresponds to increased fluorescence, and is presumably more extensive as $\dot{\gamma}$ increases, rather than decreasing slightly as seen here.

This experiment therefore finds no evidence of shear denaturation of the cytochrome c at shear rates up to $\langle \dot{\gamma} \rangle \approx 2 \times 10^5\ s^{-1}$. The cytochrome c shows essentially the same behavior as the control; its fluorescence at low and high shear rates differs by ~1% or less.

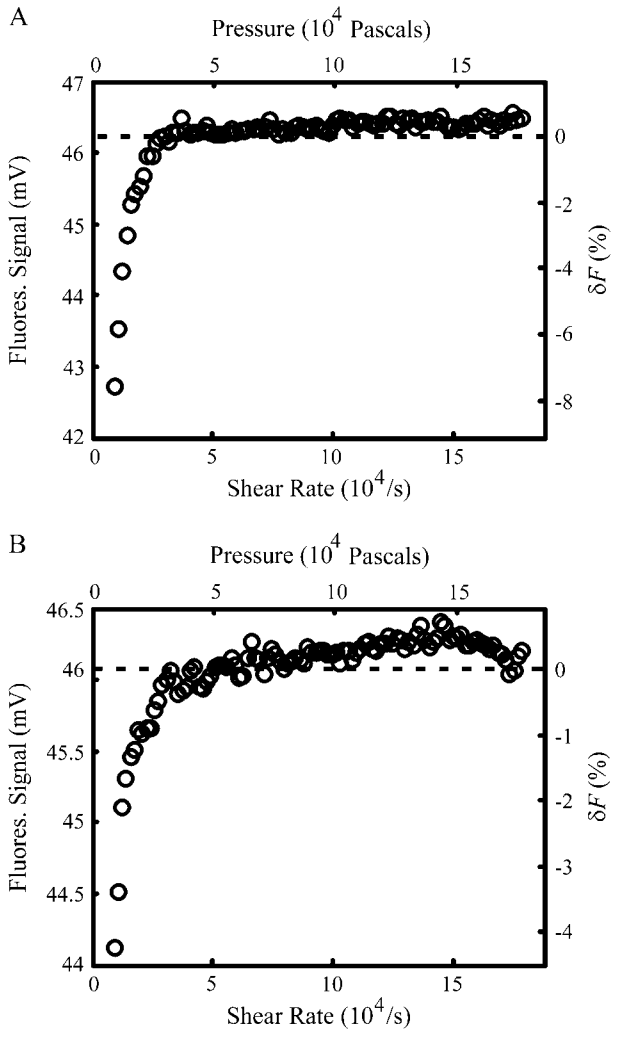

FIGURE 6 Fluorescence of (*A*) tryptophan (NATA) control sample and (*B*) cytochrome c, versus driving pressure and volume-averaged shear rate. Both samples are in 2.47 M GdnHCl, pH 5.0, citric acid buffer.

Shear-induced stretch of polymers

To consider the physics of polymer stretching and denaturation, it is useful to make the distinction between elongational and rotational flows. The gradients of a fluid velocity field $\mathbf{v}$ can be decomposed into two parts,

$$\frac{\partial v_i}{\partial x_j} = \frac{1}{2}(\omega_{i,j} + A_{i,j})$$

so as to include a rotational part

$$\omega_{i,j} = \frac{\partial v_i}{\partial x_j} - \frac{\partial v_j}{\partial x_i}$$

and an elongational part

$$A_{i,j} = \frac{\partial v_i}{\partial x_j} + \frac{\partial v_j}{\partial x_i}.$$

A shear flow is one in which only the off-diagonal components of $A_{i,j}$ are nonzero. The cylindrical laminar flow in our experimental configuration is a shear flow because the only nonzero components are

$$A_{r,z} = A_{z,r} = -\frac{\partial P}{\partial z}\frac{r}{2\eta}.$$

(These off-diagonal components give the shear rate $\dot{\gamma}$.) Flows in which the components of ω dominate are known as rotational, whereas flows in which A dominates are elongational. In the case of a simple shear flow, characterized by a spatially uniform shear rate, the magnitudes of the rotational and elongational components are equal.

Our experimental configuration does not correspond precisely to a simple shear, because the shear rate varies with r, although it does have equal rotational and elongational parts. However, a protein molecule passing through the capillary does not have time to explore different values of r and θ during the measurement; the flow in the microenvironment of each molecule is therefore virtually equivalent to simple shear, and therefore we expect the protein to respond essentially as it would in simple shear.

Should we have expected cytochrome c to unfold at shear rates exceeding 10^5 s^{-1}? As described in the Introduction, the idea that high shear can denature protein is widespread in the literature, despite rather uncertain experimental evidence. We are not aware of any theoretical work that predicts the conditions under which a protein will denature in a simple shear flow. However, the coil-stretch transition in polymers provides some useful insight into this problem.

If a polymer is placed in a sufficiently strong elongational flow, it is expected to exhibit a steep increase in its end-to-end distance, i.e., undergo a coil-stretch transition, once the velocity gradient exceeds a critical value $\sim 1/\tau_0$, where τ_0 is the longest relaxation time of the unperturbed molecule (28). However, in a rotational flow, this coil-stretch transition is not expected to occur. Interestingly, the case of simple shear (with equal rotational and elongational parts) is a marginal case: a polymer chain in a strong simple shear will not undergo the stretching transition, but exists in a state of instability (28).

This seems to argue against the complete denaturation of a protein by a simple shear flow. However, it is also true that a polymer chain in a strong simple shear is subject to large fluctuations in its end-to-end distance. The elongational component of the flow induces a stretching, whereas the rotational component turns the molecule and allows it to relax back to its compact state. These fluctuations and other dynamics have been observed in individual molecules of λ DNA in steady shear flow (29,30). They include transient extensions of the polymer and become substantial when the dimensionless Weissenberg number $Wi = \dot{\gamma}\tau_0$ exceeds (roughly) $Wi \sim 5$.

The behavior of simple long polymers therefore suggests that simple shear could induce large fluctuations—rapid folding and unfolding transitions—in a protein once $\dot{\gamma}\tau_0$ exceeds unity, where τ_0 is the folding timescale. This would imply that the many proteins with millisecond (or slower) folding kinetics could be destabilized by easily attainable velocity gradients of $\sim 10^3$ s^{-1} or less. For the *U-I* transition in cytochrome c, τ_0 would be the equilibration time (~ 50 μs) for that transition, and so gradients of $\sim 10^4$ s^{-1} would be necessary. In fact, however, our study finds no evidence that the *U-I* transition in cytochrome c is influenced by shear rates as high as $\langle \dot{\gamma} \rangle \approx 2 \times 10^5$ s^{-1}, corresponding to $Wi \approx 10$.

Therefore, although the behavior of long-chain polymers provides some insight into the problem, the question remains: why does even a high rate of shear appear insufficient to denature a small, globular protein? We present below a simple toy model to suggest that the free energy cost of unfolding the native structure of the protein—a cost largely absent in the coil-stretch transition of a homopolymer—raises the threshhold $\dot{\gamma}$ to an extraordinarily large value that will rarely be attainable in laminar flow studies.

Simple model for protein denaturation in elongational flow

We treat the protein molecule as a necklace of N spherical beads, where the center-to-center distance between consecutive beads is $d = 3.8$ Å. We make the simple approximation that, under the influence of a strongly elongational flow with $\dot{\gamma} = dv_x/dx$, the protein begins to denature by dividing into two roughly spherical clusters of radius a (Fig. 7). The clusters are separated by a linker of n beads oriented parallel to the x axis. Each cluster therefore contains $(N - n)/2$ beads and has volume $(4/3)\pi a^3 = (N - n)v_b/2$. Here, v_b is the average volume occupied by one bead ($v_b \approx 1.5 \times 10^{-28}$ m^3 if one bead equals one amino acid in cytochrome c). For a strongly elongational flow, the protein experiences a difference $(v_2 - v_1) = \dot{\gamma}\, nd$ in the flow velocities v_1 and v_2 at the two clusters. The resulting difference in the viscous force on the two clusters creates a tension in the linker,

$$T \approx 6\pi\eta a(v_2 - v_1)/2 = 3\pi\eta a\,\dot{\gamma}\, nd.$$

As the two clusters separate and the linker grows, the tension varies with n:

$$T = 3\pi\eta\,\dot{\gamma}\, nd(3v_b(N - n)/(8\pi))^{1/3}.$$

With the extension of the linker by one bead ($\delta n = 1$) the viscous force does work $\delta W = T\delta x = Td\delta n$. The net work done by the fluid in completely separating the two clusters is

$$W = 3\pi\eta\,\dot{\gamma}\, d^2\left(\frac{3v_b}{8\pi}\right)^{1/3}\int_0^N ndn(N - n)^{1/3}$$
$$= (27/28)\pi\eta d^2\,\dot{\gamma}\, N^{7/3}(3v_b/8\pi)^{1/3}.$$

In a two-state model for folding/unfolding, the protein unfolds when the work done equals the thermodynamic stability ΔG of the folded state, or ~ 42 kJ/mol for cytochrome

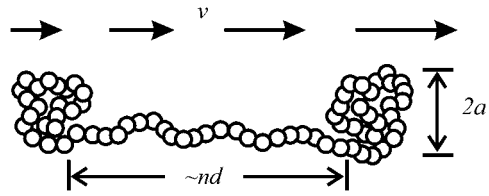

FIGURE 7 Elementary model for shear denaturation of a protein by an elongational flow: a protein of N residues (small spheres, with center-to-center separation d) divides into two clusters of residues, separated by a linker of $\sim n$ residues and length $\sim nd$. The heterogeneity of the velocity field $\mathbf{v}$ leads to a tension in the linker.

c with $N \approx 104$ amino acids. Defining $\Delta = \Delta G/N \approx 0.40$ kJ/mol/residue $\approx 7 \times 10^{-22}$ J/residue, we have unfolding when $W \approx N\Delta$ or

$$\dot{\gamma} \approx \Delta/(\pi\eta d^2 N^{4/3}(3v_b/8\pi)^{1/3}).$$

For a chain of $N = 100$ residues in water, this predicts a very large value, $\dot{\gamma} \approx 10^7\ s^{-1}$. Further, the model makes the optimistic assumption of a purely elongational flow and ignores the entropic restoring force within the linker. This suggests that an even larger shear rate might be required to significantly unfold a real protein. (Of course, a more sophisticated model would take account of the activated nature of the unfolding dynamics, the role of the shear in reducing the activation free energy, rotational components to the flow, etc.)

Attaining a simple shear rate of $\sim 10^7\ s^{-1}$ in water, under laminar flow conditions, would require, e.g., $v \approx 100$ m/s in a capillary of radius $R = 10\ \mu$m (e.g., $v/R \approx 10^7\ s^{-1}$ with $Re = \rho vR/\eta \leq 10^3$). This in turn requires a very large driving pressure gradient $\sim 4\eta v/R^2 \approx 4 \times 10^9$ Pa $m^{-1} = 580$ psi/mm (Eq. 1). Clearly, our simple model suggests that small proteins are exceedingly unlikely to shear-denature in any reasonably attainable laminar flow, except perhaps in solvents of very high viscosity (which reduce the magnitude of $\dot{\gamma}$ needed).

The above model assumes that the protein has native-like stability $\Delta G \approx N\Delta$. If the shear is applied under solvent conditions that place the protein near or beyond the midpoint of the denaturation transition—as in our 2.5 M GdnHCl experiment—where ΔG is very small or even negative, the model predicts that unfolding should occur at more modest $\dot{\gamma}$. We did not observe such unfolding either at the pH 5.0 denaturation midpoint (2.5 M GdnHCl) or at the pH 7.0 denaturation midpoint (2.8 M GdnHCl). This puzzling result invites future experimental and theoretical investigation.

An alternative theoretical model is simply to suggest that the normal unfolded configurations of a protein are not sufficiently extended (e.g., in radius of gyration) relative to native states, and therefore they are not strongly favored in typical shear flows. Strong shear instead favors stretching of an already unfolded protein; this results in a much larger degree of extension, although (as a coil-stretch transition) it requires that the shear rate exceed the longest relaxation time of the unfolded chain, $\dot{\gamma} > 1/\tau_0$. In this sense, shear would not directly denature a protein, but it could drive a coil-stretch transition in those molecules that already happen to be unfolded. The U state is depopulated in favor of the stretched state, and so more N unfolds to restore the N-U equilibrium. The relevant relaxation time would presumably be the Zimm time of the polypeptide chain, or ~ 100 ns for cytochrome c (31). Unfolding cytochrome c in water would therefore require a shear rate $\dot{\gamma} > (100\ \text{ns})^{-1} = 10^7\ s^{-1}$. Since this gives the same high estimate for $\dot{\gamma}$ as obtained above, we conclude that the likelihood of shear unfolding a small globular protein in water is rather poor.

CONCLUSIONS

Despite a long history and a fairly large body of experimental work, the question of whether a highly shearing flow will denature a globular protein has remained unresolved. We have subjected a small protein to a very high rate of shear ($\dot{\gamma} > 10^5\ s^{-1}$), under well-defined flow conditions, and we see no evidence that the shear destabilizes the folded or compact configurations of the molecule. Although this is surprising in light of the history of reports of denaturation, an elementary model suggests that the thermodynamic stability of the protein presents a major obstacle to shear unfolding: the model predicts that only an extraordinarily high shear rate ($\sim 10^7\ s^{-1}$) would suffice to destabilize a typical small protein of ~ 100 amino acids in water. An even simpler argument based on the dynamics of the unfolded polymer leads to a similar high estimate for $\dot{\gamma}$. Such shear rates would be very difficult to attain in laminar flow; this leads to the general conclusion that shear denaturation of a small protein would require truly exceptional flow conditions. This conclusion is consistent with the existing literature, which contains only very weak evidence for denaturation of small proteins by strong shears in aqueous solvent. The few unambiguous cases of shear effects involved very unusual circumstances, such as a very high-molecular-weight protein (16) or a high solvent viscosity that resulted in an extraordinarily high shear stress (5). One may, however speculate that protein denaturation could still occur in highly turbulent flow; if so, this could have consequences for the use of turbulent mixing devices in the study of protein folding dynamics (32,33). The required shear rate also decreases with increasing protein molecular weight and solvent viscosity; denaturation in laminar flow might be possible at moderate shear rates in sufficiently large, multimeric proteins (e.g.,$\dot{\gamma} \approx 10^3\ s^{-1}$ for molecular weight $\sim 2 \times 10^7$ in water (16)) or in very viscous solvents like glycerol.

Finally, our experiments do not address the effects of shear under unfolding conditions, where the free energy of unfolding is negative: our model implies that the behavior in that case would be quite different. This may be an interesting area for future experiments. A more thorough theoretical analysis of the effects of shear on folded proteins would certainly be quite interesting.

APPENDIX: PHOTOBLEACHING

One does not anticipate observing any effect of pressure or $\dot{\gamma}$ on the fluorescence of the NATA control; the initial rapid rise in the fluorescence of the control in Figs 4 and 6 (*upper panels*) therefore suggests that the tryptophan is photobleached by the intense UV excitation laser. Tryptophan is known for its poor photostability, with each molecule emitting roughly two fluorescence photons before photobleaching occurs (34): We can roughly estimate the photodamage cross section as one-tenth of the absorbance cross section, $\sigma \approx (0.1) \times \varepsilon \ln(10)/N_A \approx 2 \times 10^{-18}\ cm^2$, where $\varepsilon \approx 5000/M\ cm = 5 \times 10^6\ cm^2$/mole is the extinction coefficient at 266 nm. The laser focus ($I \approx 20\ W/cm^2$) would then destroy a stationary tryptophan sidechain on a timescale roughly $\tau \sim hc/\sigma\lambda I \approx 20$ ms. At low flow rates, where molecules dwell in the

laser focus for many milliseconds, we expect to observe weakened emission. As the flow rate increases, the molecules spend less time in the laser focus, resulting in higher average fluorescence. We present here a simple model and fit that appear to describe this photobleaching effect.

If the tryptophan fluorophore has a lifetime τ under exposure to the laser, then the fluorescence of the average tryptophan molecule after an exposure time t is

$$F(t) = F_0 \exp(-t/\tau),$$

where F_0 is a constant. If we approximate the laser focus as a region of uniform beam intensity, extending from $z = -h/2$ to $z = +h/2$ along the flow channel, then fluorophores at coordinates (r,z) inside the channel have accumulated an exposure time $t(r,z)$ that is determined by the flow velocity of the solution $v_z(r)$:

$$t = (z + h/2)/v_z(r),$$

$$v_z(r) = v_0(R^2 - r^2)/R^2,$$

where R is the capillary radius and v_0 is controlled by the driving pressure, viscosity, etc. (Eq. 1). The fluorescence of those molecules is then

$$F(r,z) = F_0 \exp\left(-\frac{(z + \frac{h}{2})R^2}{v_0\tau(R^2 - r^2)}\right).$$

The photomultiplier detects light emitted from a short segment of the capillary within the laser focus $-d/2 \le z \le d/2$, with $d = 0.4$ mm. Then the total fluorescence collected by the photomultiplier is

$$F_{\text{Total}} = c\int_{-d/2}^{d/2} dz \int_0^R F(r,z)2\pi r dr, \qquad (3)$$

where c is the efficiency of the light collection optics. The integration can be performed numerically and fit to the experimental data, subject to the free parameters cF_0, h, and τ. (Other parameters such as d, R, and v_0 are known.)

Fig. 8 shows the data from a control sample (capillary 1) together with a least-squares fit to Eq. 3. Data and fit are in good agreement. The fit gives very reasonable values $\tau = 9.3$ ms and $h = 0.45$ mm, consistent with our estimated millisecond bleaching rate for the fluorophore as it passes through the slightly defocused laser beam. Although fairly crude (i.e., ignoring details such as the true near-Gaussian beam-intensity profile, heterogeneous bleaching due to absorbance of UV by the sample, etc.), the model provides a satisfactory fit to the data. A more sophisticated analysis is also possible, at the cost of introducing more parameters and details, but this does not seem necessary: the simple analysis confirms that the fluorescence changes observed in both the sample and control (Figs. 4 and 6) can be attributed to photobleaching of the tryptophan by the excitation laser rather than to ''interesting'' shear-induced dynamics in either the protein or the control. (Much less photobleaching is expected for the folded protein of Fig. 4 *B*, owing to the rapid Forster transfer of excitation energy to the heme.)

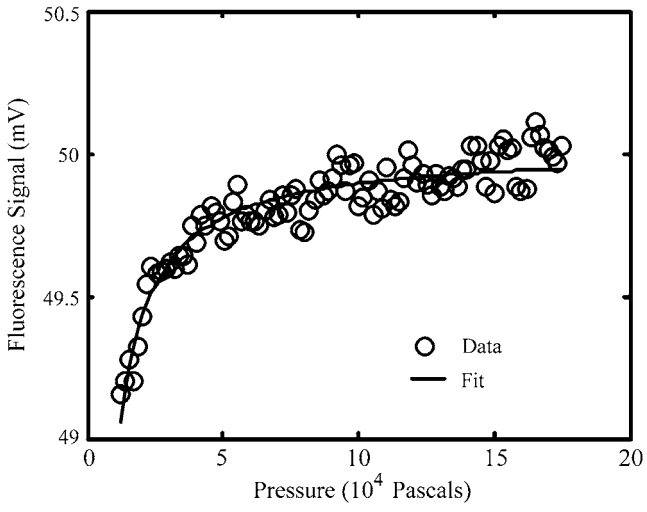

FIGURE 8 Fluorescence of tryptophan (NATA) control sample versus driving pressure (capillary 1, *open circles*), and least-squares fit (*solid line*) to photobleaching model of Eq. 3.

The authors thank Prof. Robert J. Cohen and Prof. Sergei Obukhov for interesting discussions.

Funding support was provided by the National Science Foundation, MCB 0347124, and by the University of Florida Center for the Condensed Matter Sciences.

REFERENCES

1. Creighton, T. E. 1992. Protein Folding. W. H. Freeman, New York.
2. Franks, F. 1993. Protein Biotechnology: Isolation, Characterization, and Stabilization. Humana Press, New York.
3. Bummer, P. M., and S. Koppenol. 2000. Chemical and physical considerations in protein and peptide stability. *In* Protein Formulation and Delivery. Eugene McNally, editor. Marcel Dekker, New York.
4. Constantinescu, V. N. 1995. Laminar Viscous Flow. Springer-Verlag, New York.
5. van der Veen, M. E., D. G. van Iersel, A. J. van der Goot, and R. M. Boom. 2004. Shear-induced inactivation of α-amylase in a plain shear field. *Biotechnol. Prog.* 20:1140–1145.
6. Charm, S. E., and B. L. Wong. 1970. Enzyme inactivation with shearing. *Biotechnol. Bioeng.* 12:1103–1109.
7. Charm, S. E., and B. L. Wong. 1970. Shear degradation of fibrinogen in circulation. *Science.* 170:466–468.
8. Charm, S. E., and B. L. Wong. 1975. Shear inactivation of heparin. *Biorheology.* 12:275–278.
9. Charm, S. E., and B. L. Wong. 1975. Shear degradation of heparin. *Biorheology.* 12:93. (Abstr.)
10. Charm, S. E., and B. L. Wong. 1981. Shear effects on enzymes. *Enzyme Microb. Technol.* 3:111–118.
11. Tirrell, M., and S. Middleman. 1975. Shear modification of enzyme-kinetics. *Biotechnol. Bioeng.* 17:299–303.
12. Thomas, C. R., A. W. Nienow, and P. Dunnill. 1979. Action of shear on enzymes - studies with alcohol-dehydrogenase. *Biotechnol. Bioeng.* 21:2263–2278.
13. Thomas, C. R., and P. Dunnill. 1979. Action of shear on enzymes: studies with catalase and urease. *Biotechnol. Bioeng.* 21:2279–2302.
14. Maa, Y. F., and C. C. Hsu. 1996. Effect of high shear on proteins. *Biotechnol. Bioeng.* 51:458–465.
15. Maa, Y. F., and C. C. Hsu. 1997. Protein denaturation by combined effect of shear and air-liquid interface. *Biotechnol. Bioeng.* 54:503–512.
16. Siedlecki, C. A., B. J. Lestini, K. K. Kottke-Marchant, S. J. Eppell, D. L. Wilson, and R. E. Marchant. 1996. Shear-dependent changes in the three-dimensional structure of human von Willebrand factor. *Blood.* 88:2939–2950.
17. Lee, A. T., and A. J. McHugh. 1999. The effect of simple shear flow on the helix-coil transition of poly-L-lysine. *Biopolymers.* 50:589–594.
18. Oliva, A., A. Santovena, J. Farina, and M. Llabres. 2003. Effect of high shear rate on stability of proteins: kinetic study. *J. Pharm. Biomed. Anal.* 33:145–155.
19. Lemak, A. S., J. R. Lepock, and J. Z. Y. Chen. 2003. Molecular dynamics simulations of a protein model in uniform and elongational flows. *Proteins.* 51:224–235.

20. Tu, R. S., and V. Breedveld. 2005. Microrheological detection of protein unfolding. *Phys. Rev. E.* 72:041914.

21. Shastry, M. C. R., and H. Roder. 1998. Evidence for barrier-limited protein folding kinetics on the microsecond time scale. *Nat. Struct. Biol.* 5:385–392.

22. van der Meer, B. W., G. Coker, and S.-Y. Chen. 1994. Resonance Energy Transfer: Theory and Data. Wiley-VCH, New York.

23. Elove, G. A., A. K. Bhuyan, and H. Roder. 1994. Kinetic mechanism of cytochrome-*c* folding: involvement of the heme and its ligands. *Biochemistry.* 33:6925–6935.

24. Hagen, S. J., R. F. Latypov, D. A. Dolgikh, and H. Roder. 2002. Rapid intrachain binding of histidine-26 and histidine-33 to heme in unfolded ferrocytochrome *c*. *Biochemistry.* 41:1372–1380.

25. Kawahara, K., and C. Tanford. 1966. Viscosity and density of aqueous solutions of urea and guanidine hydrochloride. *J. Biol. Chem.* 241: 3228–3232.

26. Pascher, T. 2001. Temperature and driving force dependence of the folding rate of reduced horse heart cytochrome *c*. *Biochemistry.* 40: 5812–5820.

27. Segel, D. J., A. L. Fink, K. O. Hodgson, and S. Doniach. 1998. Protein denaturation: a small-angle X-ray scattering study of the ensemble of unfolded states of cytochrome *c*. *Biochemistry.* 37:12443–12451.

28. Degennes, P. G. 1974. Coil-stretch transition of dilute polymers under ultrahigh velocity-gradients. *J. Chem. Phys.* 60:5030–5042.

29. Smith, D. E., H. P. Babcock, and S. Chu. 1999. Single-polymer dynamics in steady shear flow. *Science.* 283:1724–1727.

30. Leduc, P., C. Haber, G. Bao, and D. Wirtz. 1999. Dynamics of individual flexible polymers in a shear flow. *Nature.* 399: 564–566.

31. Qiu, L. L., C. Zachariah, and S. J. Hagen. 2003. Fast chain contraction during protein folding: ''foldability'' and collapse dynamics. *Phys. Rev. Lett.* 90:168103.

32. Shastry, M. C. R., S. D. Luck, and H. Roder. 1998. A continuous-flow capillary mixing method to monitor reactions on the microsecond time scale. *Biophys. J.* 74:2714–2721.

33. Roder, H., K. Maki, H. Cheng, and M. C. R. Shastry. 2004. Rapid mixing methods for exploring the kinetics of protein folding. *Methods.* 34:15–27.

34. Lippitz, M., W. Erker, H. Decker, K. E. van Holde, and T. Basche. 2002. Two-photon excitation microscopy of tryptophan-containing proteins. *Proc. Natl. Acad. Sci. USA.* 99:2772–2777.